C S S A

CENTER FOR SPACE SCIENCE AND ASTROPHYSICS
STANFORD UNIVERSITY
Stanford, California

THE DEVELOPMENT AND TEST OF

MULTI-ANODE MICROCHANNEL ARRAY DETECTOR SYSTEMS

II. SOFT X-RAY DETECTORS

Progress Report for NASA Grant NAG5-622
for the period 1 August 1985 to 31 January 1986

J. G. Timothy
Principal Investigator

Center for Space Science and Astrophysics
Stanford University
Stanford, California 94305

During the past six months efforts continued to be concentrated on the evaluation of the high-gain curved-channel MCPs at soft x-ray wavelengths. The ultra-high vacuum calibration facility with the florescent soft x-ray sources was brought into operation and the initial data on MCP gain and resolution as a function of photon energy were recorded. Initial tests are being undertaken using 25-micron pore size curved-channel MCP in order to obtain a full understanding of how the system operates. Some improvements to the system have already been identified and will be implemented shortly. The Residual Gas Analyzer (RGA) has been added to the calibration facility and has been interfaced to the HP minicomputer. Quantitative measurements of the outgassing from the MCPs during bake and evaluation has now started.

In parallel, the curved-channel MCP with a curved front face has been baked and is now being installed on the imaging (1 x 100)-pixel system in order to complete the detailed evaluation.

A series of discussions have been held with EMR Photoelectric about the appropriate means for processing CsI photocathodes to produce a high quantum yield at extreme ultraviolet (EUV) and soft x-ray wavelengths. We are designing a demountable tube structure which will incorporate a Residual Gas Analyzer (RGA) head to fully quantify the internal conditions within the tube prior to deposition of the CsI.

A detailed review paper on "Microchannel plates and image detection at soft x-ray wavelengths" was presented at the SPIE 2nd International Symposium that was held December 2-6, 1985, in Cannes, France. A copy of the galley of this paper is attached to this progress report.

An investigation of the performance characteristics of a totally new type of high-gain MCP, namely the off-axis channel MCP fabricated by Detector Technology Inc., was begun during this period. This MCP which employs a helix configuration of the channel offers the prospect of performance characteristics that are equivalent or superior to those of the curved-channel "C-plate" MCPs. However, the "off-axis channel" MCP is significantly easier to fabricate. Of particular importance for soft x-ray astrophysics is the possibility of fabricating extremely large high-gain MCPs for imaging wide-field detector systems.

Attachment:

"Microchannel plates and image detection at soft x-ray wavelengths" by J. G. Timothy.

Microchannel Plates and Image Detection at Soft X-ray Wavelengths

J. G. Timothy

Center for Space Science and Astrophysics
Stanford University, ERL 314
Stanford, California 94305, USA

Abstract

Detector systems based on the high-gain microchannel plate (MCP) electron multiplier have been used extensively for imaging at soft x-ray wavelengths both on the ground and in space. The latest pulse-counting electronic readout systems provide zero readout-noise, spatial resolutions (FWHM) of 25 microns or better and can determine the arrival times of detected photons to an accuracy of the order of 100 ns. These systems can be developed to produce detectors with active areas of 100 mm in diameter or greater. The use of CsI photocathodes produces very high detective quantum efficiencies at wavelengths between about 100 and 1Å (~0.1 to 10 keV) with moderate energy resolution. The operating characteristics of the different types of soft x-ray MCP detector systems are described and the prospects for future developments are discussed.

Introduction

The development of the high-gain microchannel plate (MCP) electron multiplier has made possible the fabrication of high-sensitivity, large-format imaging detectors for use at soft x-ray wavelengths between about 100Å and 1Å (~0.1 to 10 keV). A number of position-sensitive electronic readout systems have been developed which can directly detect the charge pulse from the output face of the MCP. The ability of the high-gain MCP to operate stably in an open-structure mode in a high-vacuum environment and the intrinsic simplicity and rugged nature of these detector systems makes them particularly suitable for use in space astrophysics instruments. In this paper the current state-of-development of the high-gain MCPs and the performance characteristics of the different types of readout systems are reviewed. The configurations of the different soft x-ray photocathodes are described and the differences in the operating characteristics of the MCP detectors and the solid-state CCD detectors at soft x-ray wavelengths are briefly compared. The prospects for the future development of the MCP detectors are discussed.

High-gain Microchannel Plates (MCPs)

The microchannel plate (MCP) operates in an identical manner to that of the conventional channel electron multiplier (CEM) which consists of a semi-conducting glass channel having an internal diameter of a few millimeters and a length-to-diameter ratio of the order of 100:1. In operation, a potential of about 2000 V is applied along the length of the channel when the CEM is in a high-vacuum enclosure. An electron released from the wall of the channel at the input by the impact of either a photon or a charged particle is accelerated along the channel axis and drifts across to strike the wall with sufficient energy to release secondary electrons (see Figure 1a).

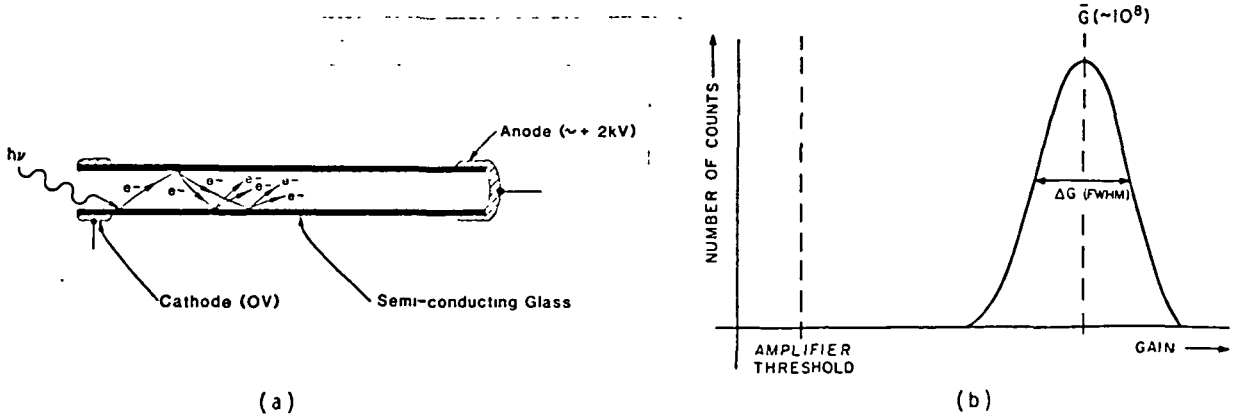

Figure 1. The Channel Electron Multiplier (CEM).

a. Mode of operation. b. Form of output pulse-height distribution.

The process is repeated throughout the length of the channel, and the output charge pulse, normally containing 10^6 to 10^8 electrons, is collected at the anode. The channel of a high-gain CEM is curved to inhibit the acceleration of positive ions produced by the impact of electrons with residual gas molecules towards the cathode where they can initiate secondary avalanches producing a noisy and unstable device.

At high gain the amplitude of the output pulse is clipped by the effects of space charge within the channel, and the output pulse-height distribution has the saturated form shown in Figure 1b. The resolution of the output pulse-height distribution can be defined as

$$R = \Delta G/\bar{G}$$

where ΔG equals the full width at the half height of the distribution and $\bar{G}$ equals the modal gain value. Resolutions of the order of 30 to 50% are typically obtained.

Since the performance of the CEM depends principally on the length-to-diameter ratio of the channel and on the applied potential and not on the absolute physical dimensions, the CEM can be reduced to a size set by the limitations of glass fiber technology, using techniques as described, for example, by Wiza[1]. The microchannel plate (MCP) consists of a glass disk composed of several million of these small channels each of which can act as an independent electron multiplier. Typical channel diameters range from 8 to 25 microns and channel length-to-diameter ratios from about 40:1 to 140:1, yielding a plate thickness of the order of 1 to 2 mm. The MCP is thus a highly compact electron multiplier with a two-dimensional imaging capability. Until recently, MCPs could only be fabricated with straight channels and a single MCP was susceptible to ion-feedback instabilities when operated at gains above about 10^4 electrons pulse^{-1}. However, MCPs can be fabricated with the channels set at a bias angle with respect to the face of the plate and a multiplier can be constructed from two or more MCPs with suitable bias angles and plate orientations so that positive ions are trapped near the plate intersections. The configurations of these "Chevron" and "Z-plate" multipliers are shown in Figures 2a and b. The total voltage across the MCP stack can then be increased to the level at which a stable high-gain and a saturated output pulse-height distribution are obtained.

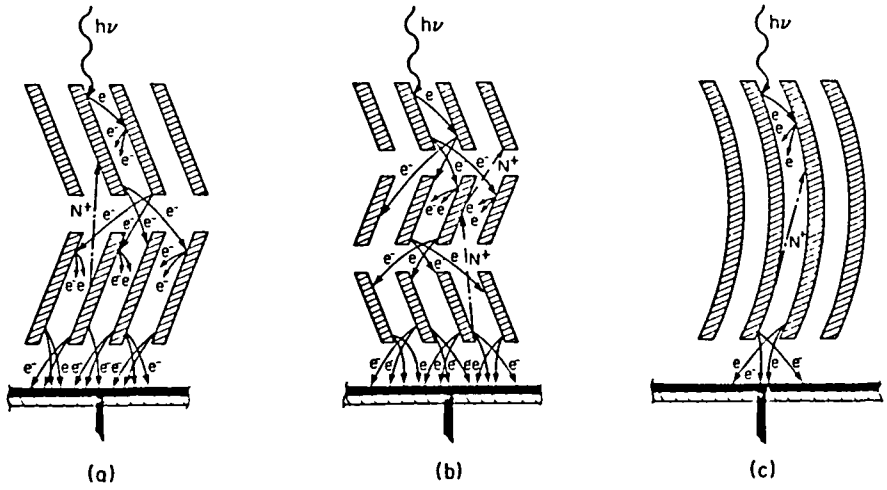

Figure 2. Configurations of high-gain MCPs.

a. "Chevron" MCP. b. "Z-plate" MCP. c. "C-plate" MCP.

The trapping of positive ions in a "Chevron" or "Z-plate" MCP is generally not as effective as in a curved CEM and the output pulse-height distributions from these MCPs have tended to be rather broad (resolutions 100%). However, a number of investigators[2,3] have reported on improved performance when the "Chevron" or "Z-plate" is constructed from MCPs having long length-to-diameter ratios of the order of 80:1 to 120:1. Resolutions of 40 to 60% have been obtained with these MCPs at gains in excess of 10^7 electons pulse^{-1}.

The recent fabrication of "C-plate" MCPs in which the channels are curved to inhibit ion-feedback in an identical manner to that employed in a CEM (see Figure 2c) has accordingly significantly improved the performance characteristics of a single MCP.[4] These curved-channel MCPs (Figure 3) have demonstrated gains of greater than 10^6 electrons pulse^{-1}, resolutions of the output pulse-height distribution of 40% or better (see Figure 4) and a stable response to accumulated signal levels in excess of 2.5×10^{11} counts mm^{-2}.

Timothy

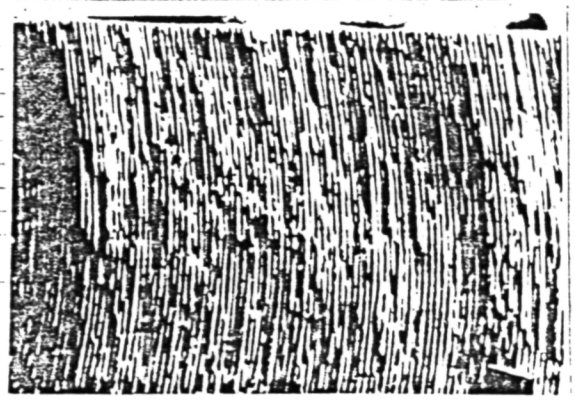

Figure 3. Section of curved-channel MCP.

A number of parameters clearly indicate that the suppression of ion-feedback in the curved-channel MCPs is more effective than in the "Chevron" or "Z-plate" MCPs. First, the very low dark count rate even when operated at ambient pressures of the order of 10^{-5} Torr, critically important for the use of the MCPs in open-structure soft x-ray detectors on orbiting spacecraft. Second, the very low tail of high-amplitude pulses in the output pulse-height distribution (see Figure 4). Third, the stable operation of a curved-channel MCP with the front face curved to match the curved focal surface of a grazing-incidence telescope or spectrometer. This MCP (Figure 5) has the front face curved to a radius-of-curvature of 250 mm and a planar output face, yielding a variation in the length-to-diameter ratios of the channels from 140:1 at the edge to 110:1 at the center of the active area. Preliminary test results show stable operation free of ion-feedback anywhere in the active area at gains in excess of 7×10^5 electrons pulse^{-1}.

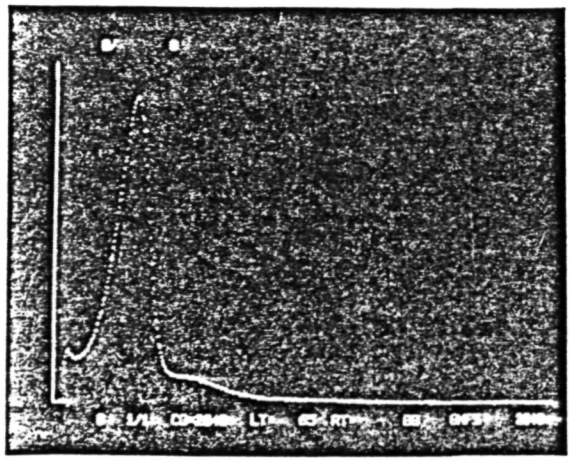

Figure 4. Output pulse-height distribution for a curved-channel MCP with 25-micron-diameter channels. Modal gain 1.3×10^6 electrons pulse^{-1}. Resolution 40% (FWHM).

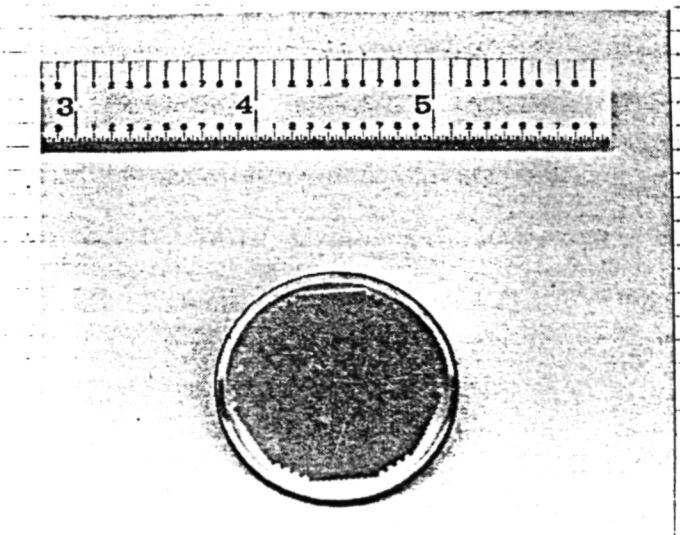

Figure 5. Curved-channel MCP with front face curved to a radius-of-curvature of 250 mm.

One of the major advantages of the MCP as an imaging electron multiplier is the available size. Straight channel MCPs are available with 12-micron-diameter channels and active areas larger than 130 mm in diameter and can be "slumped" to provide a steeply curved focal surface (see Figure 6). Curved-channel MCPs are currently available from Galileo Electro-Optics Corporation[5] with 12-micron-diameter channels and active areas of up to 75 mm in diameter. 25-mm-and 40-mm-format curved-channel MCPs have also been fabricated with rectangular and square active areas to match the active areas of specific readout systems (see Figure 7).

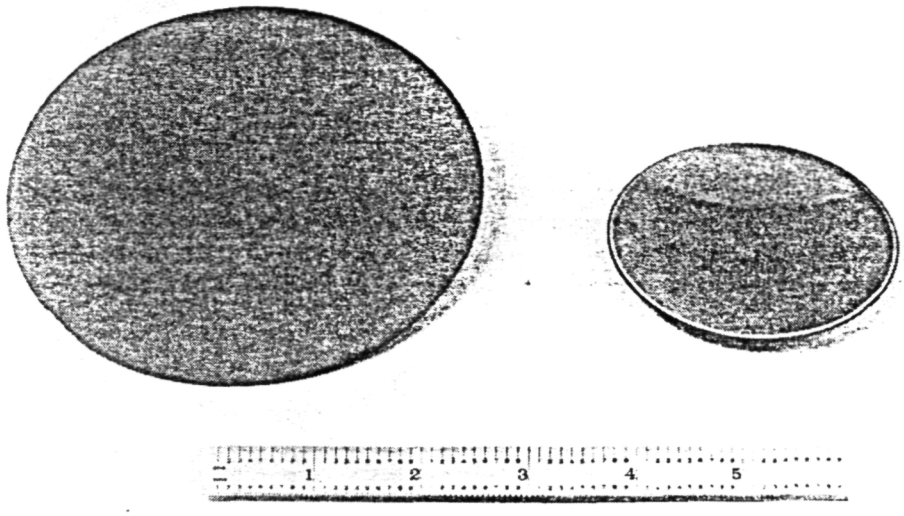

Figure 6. 130-mm diameter planar MCP and 75-mm-diameter "slumped" MCP with curved focal surface.

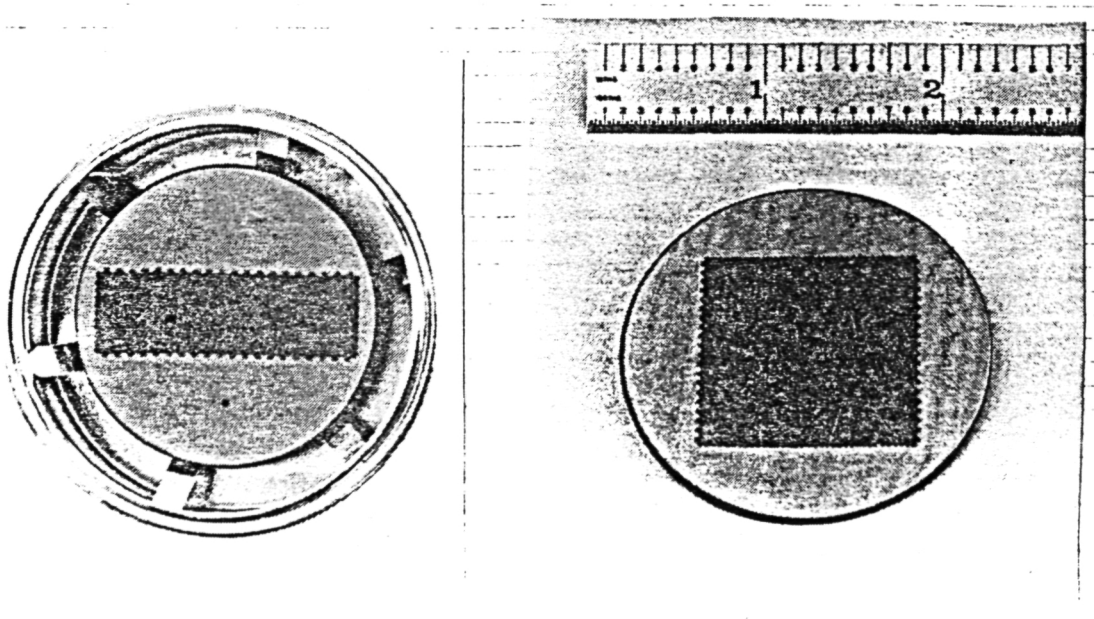

(a) (b)

Figure 7. Curved-channel MCPs with active areas tailored to match the active areas of the readout arrays.

a. 7 x 27 mm^2 active area for a (256 x 1024)-pixel readout array.
b. 27 x 27 mm^2 active area for a (1024 x 1024)-pixel readout array.

Electronic Readout Systems

In the simplest type of electronic readout system the charge pulse from the MCP is accelerated onto a visible-light phosphor and the intensified image detected by a photosensitive array such as a silicon diode array (for example, an E. G. and G. Reticon array[6]) or a CCD (see Figure 8a).

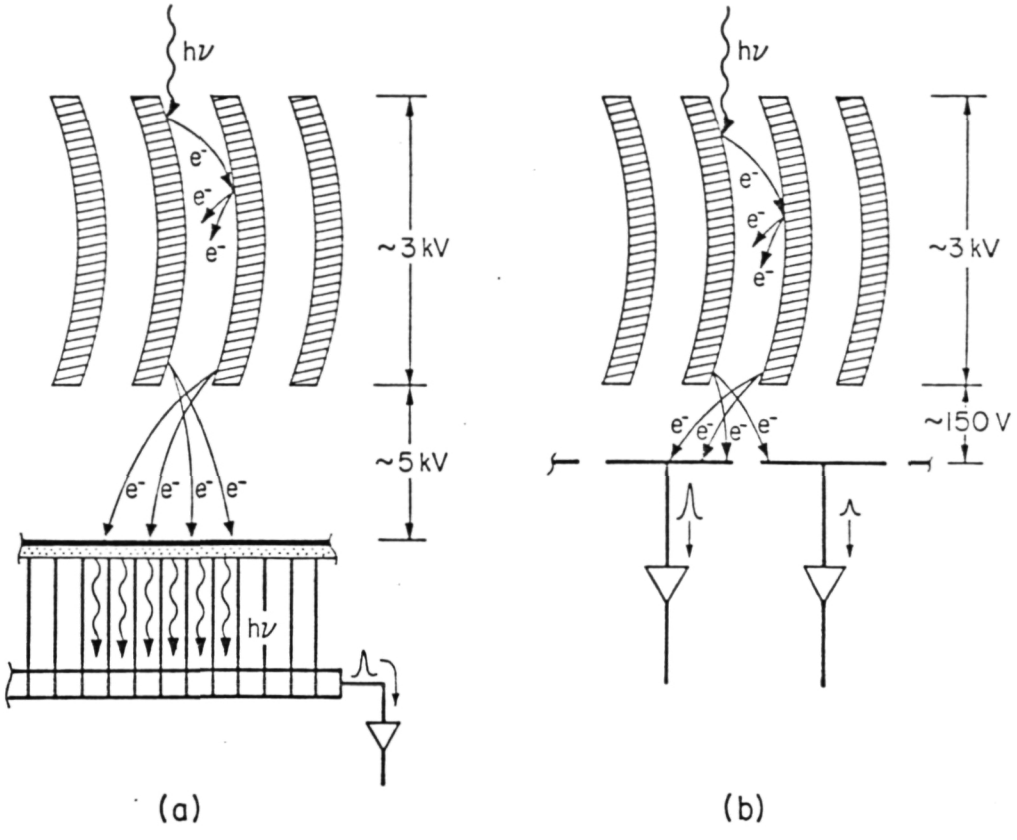

Figure 8. High-gain MCP readout systems.

a. Intensified photoconductive array.
b. Multi-anode array.

With an MCP gain of the order of 10^4 to 10^5 electrons pulse^{-1} and an additional gain in the phosphor of 10 sufficient photons can be fiber-optically coupled to the diode array or CCD to produce enough charge in the depletion region for single photon detection.[7,8] The principal advantage of the intensified photoconductive array is that it can be assembled from readily available off-the-shelf components. However, the intensified photoconductive array has a number of significant disadvantages for high-energy astrophysics studies in space.

First, light spreading at the phosphor and in the optical coupling system causes the size of the light spot to be significantly greater than the size of the diodes (i.e., pixels) in the Reticon array or CCD. However, centroiding techniques can be used to identify the location of the center of the light pulse to an accuracy of a fracton of a diode, as described by Stapinski et al.[9] and Latham.[10] A further complication is caused by the phosphor decay time which is sufficiently long that, at typical array readout rates, the light pulse from a single event may be detected on more than one readout cycle. In order to overcome this problem prior-frame subtraction techniques are used (see, for example, Gorham, Rodgers, and Stapinski.)[11] Because of the phosphor decay time and because of the size of the light pulse, the dynamic range of an Intensified Photoconductive array is dependent on the type of image being recorded. For flat-field imaging or for recording stellar spectra a count rate of the order of 1 to 5 counts diode^{-1}s^{-1} (random) will typically produce a 10% coincidence loss. However, for isolated strong emission lines, such as obtained from spectrograph calibration light sources, much higher local count rates can be tolerated. With correct prior-frame subtraction techniques in operation, the Intensified Photoconductive arrays will operate at very close to photon statistics noise-limited operation.

An additional disadvantage is that the serial readout from the CCD (typical frame rates ~30 Hz) reduces the timing accuracy of the system. It is thus more difficult to determine the arrival times of photons for studies of dynamic phenomena or for post facto reconstruction of the spacecraft pointing, as was done for example on the Einstein observatory. For these reasons the most commonly used MCP readout systems for high-energy astrophysics experiments are those that directly detect the output charge pulse from the MCP (see Figure 8b).

Because of the very low photon flux rates, spectroscopic or imaging instruments for astrophysics experiments typically require a large number of pixels for efficient operation. At this time, four imaging electronic readout systems are being used at extreme ultraviolet (EUV) and soft x-ray wavelengths. These are the Resistive Anode Encoder (RAE)[1,12,13] (Figure 9a), the High-Resolution Imager (HRI)[14] (Figure 9b), the Wedge-and-Strip Array (WSA)[15] (Figure 9c) and the Multi-Anode Microchannel Array (MAMA)[16] (Figure 9d).

The simplest of these systems, the Resistive Anode Encoder (RAE), employs a resistive anode to locate the event by means of charge division[17] or rise-time[18] encoding techniques. The block diagram of a one-dimensional RAE using rise-time discrimination is shown in Figure 9a. In a one-dimensional array, an amplifier is connected to each end of a resistive sheet. The output charge pulse from the MCP will be divided between the two amplifiers in proportion to the distance of the pulse from the ends of the sheet. The spatial location can accordingly be determined by ratioing the charge detected by the two amplifiers or by measuring the differences in the rise times of the two charge pulses. A two-dimensional, resistive anode array can be constructed with four amplifiers, one at each corner of the sheet. In this case the position is determined in two dimensions from the ratios of the charge detected by opposite pairs of amplifiers. One-dimensional resistive anode arrays give good spatial linearity; but two-dimensional resistive anode arrays require low resistivity borders to overcome significant image distortion caused by charge reflection effects.[19]

This very simple system has a number of limitations. First, the spatial resolution is dependent on the gain of the MCP; and for the best spatial resolutions, the RAE requires gains in excess of 10^7 electrons pulse^{-1} dictating the use of "Chevron" or "Z-plate" MCP stacks in which the charge cloud is allowed to spread over a number of channels. The best resolution obtained to date, of the order of 40 microns, requires a stack of five MCPs to produce a gain approaching 10^8 electrons pulse^{-1}. Second, the spatial resolution begins to degrade because of pulse pileup at signal levels in excess of about 10^4 counts s^{-1} (random). At high count rates the coincident arrival of pulses is interpreted by the readout electronics as a single event midway between the two simultaneous events (see, for example, Mertz et al.[20]). This causes a false image to be formed between bright areas in the detected image.

A more complex version of the RAE which uses discrete anode wires resistively coupled in sets is the High-Resolution Imager (HRI) developed by the Smithsonian Astrophysical Observatory for use as an x-ray detector on the Einstein mission. The readout technique for the HRI is shown schematically in Figure 9b. An amplifier is connected to every eighth wire with a total of 34 amplifiers used for the two-dimensional system. The amplifiers are combined into three groups, and the fine position of the centroid is determined from the division of charge among the three groups by using a cyclic algorithm of the form (A-C)/(A+B+C). The coarse position is determined by the rank of the amplifiers. The accuracy of determining the centroid is of the order of 15-30 microns (1σ fit).

The ultimate spatial resolution in the resistive anode systems will, however, be limited by thermal noise[17] and accordingly a number of centroiding systems ultilizing conducting electrodes have been developed.

The most effective of the centroiding systems in use today is the Wedge-and-Strip Array (WSA) developed by a group at the University of California, Berkeley. A schematic of a typical WSA configuration is shown in Figure 9c. In this array, charge is collected on a number of discrete conducting electrodes, but positional information is once again determined by the ratio of the charge collected on the different electrodes. In the array shown in Figure 9c, the coordinates of the event in the horizontal (X-axis) are determined by the ratio of the charge collected on electrodes C and D, and in the vertical (Y-axis) by the ratio of the charge collected on the elecrodes A and B. Two-dimensional WSAs can be constructed with only three electrodes.[2] Spatial resolutions of the order of 40 microns have been obtained with MCP gains in excess of 10^7 electrons pulse^{-1}. The optimization of large-format WSAs with active areas up to 200 mm in diameter has been discussed by Schwartz and Lapington.[21]

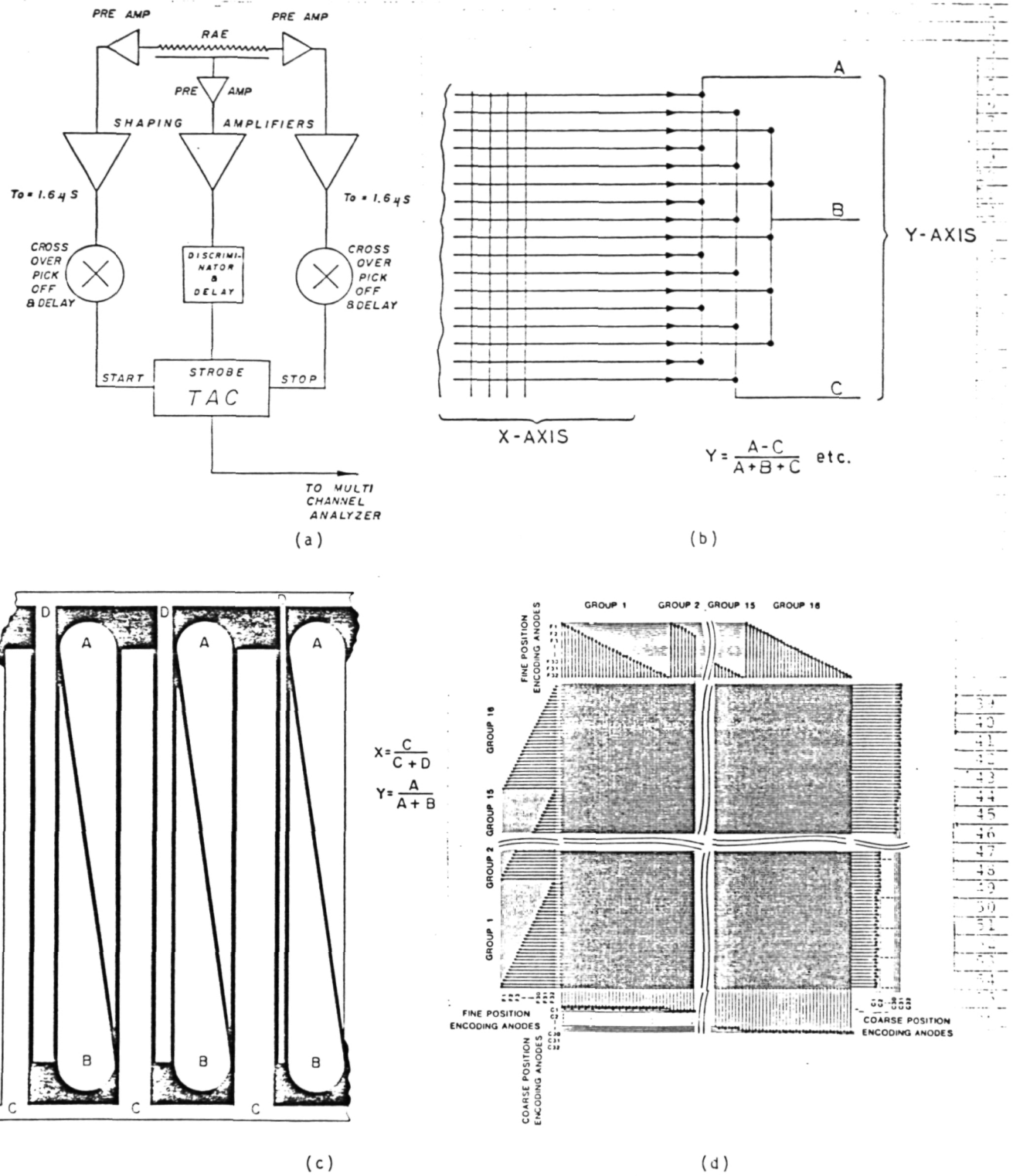

Figure 9. Electronic readout systems for high-gain MCPs.

a. Resistive Anode Encoder (from Wiza[1]).
b. High-resolution Imager (from Kellogg et al.[14]).
c. Wedge-and-strip array (from Martin et al.[15]).
d. Two-dimensional Multi-Anode Microchannel Array (from Timothy[16]).

A readout system which is designed to eliminate the high-gain requirements and the dynamic range limitations of centroiding systems and which uses a precision array of electrodes to collect the charge pulse is currently under development by the author in collaboration with Ball Aerospace Systems Division (BASD).[22] The multi-layer, coincidence-anode, Multi-Anode Microchannel Array (MAMA) (see Figure 9d) employs two sets of anodes insulated from each other but exposed to the output face of the MCP. The output charge cloud from the MCP divides between two sets of anodes in each axis at the position where the event occurs allowing the spatial location to be indentified by the coincident arrival of pulses on the appropriate pair of anodes. Photometric data from a x b pixels in each axis can then be read out with a total of a + b amplifier and discriminator circuits.[23]

Two-dimensional arrays are constructed from two identical coincidence-anode arrays arranged vertically above each other and oriented orthogonally. As shown in Figure 9d, a (1024 x 1024)-pixel array fabricated in this manner employs coincidence detection in the two axes and requires only a total of 128 amplifier and discriminator circuits. The technical problem in the fabrication of these multi-layer arrays is the need to expose the lower-layer electrodes to the low energy (order of 30 V) electrons from the MCP which cannot penetrate an insulating layer. This is accomplished by etching away the silicon dioxide insulating layer between the two sets of electrodes in the interstices between the upper-layer electrodes. The largest format coincidence anode arrays in operation today have formats of 256 x 1024 pixels and spatial resolutions of 25 x 25 microns^2 (FWHM).

A more detailed comparison of the different MCP electronic readout systems has been presented recently by the author.[24]

Soft x-ray photocathodes

The semi-conducting glass of the MCP can be used as a moderately efficient photocathode at EUV and soft x-ray wavelengths. However, at energies above about 20 eV (~500Å) the quantum efficiencies of all materials increases dramatically with the angle of illumination. For this reason MCP detector systems for use with grazing-incience optical systems typically employ channels at a 0° bias angle with the photocathode material deposited in the internal surface. Because of the strong dependance of quantum efficiency on the angle of incidence it is highly advantageous to "funnel" the inputs to the channels to increase the open area ratio and the percentage of the photocathode illuminated at high angles of incidence.

At this point in time CsI when deposited and stored under high vacuum appears to be the most efficient and readily available photocathode material for use at EUV and soft x-ray wavelengths.[25,26] Two configurations can be used, namely high-density "opaque" CsI directly deposited on the front face of the MCP (see Figure 10a) or low-density "fluffy" CsI deposited on a thin soft x-ray filter and mounted in proximity focus with the front face of the MCP (see Figure 10b). For both configurations, an appropriate focusing electrostatic field must be used to prevent degradation of the image quality by dispersion of the photoelectrons (see, for example, Taylor et al.[27])

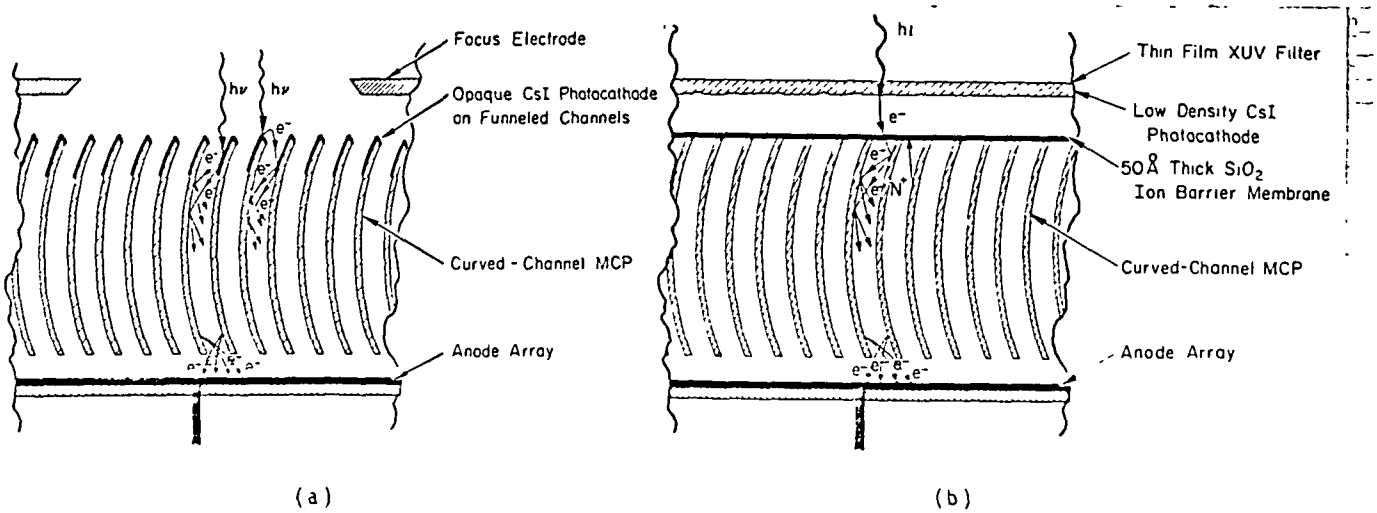

Figure 10. CsI photocathode configurations for use at soft x-ray wavelengths.

a. Opaque CsI deposited on the front face of the MCP.
b. "Fluffy" CsI mounted in proximity focus with the front face of the MCP.

A comparison of the quantum efficiencies of opaque and "fluffy" CsI photocathodes of optimum thickness illuminated at normal incidence is shown in Figure 11. However, it should be noted that significantly higher quantum efficiencies can be obtained with opaque CsI illuminated at high angles of incidence.[29,30] Higher values have also been obtained from CsI photocathodes deposited on pellicle substrates and maintained in a dry environment.[31] The importance of maintaining the CsI photocathodes in a water free environment cannot be overemphasized. Because of the dependence of the number of photoelectrons emitted from CsI on the photon energy at wavelengths below 100Å a moderate level of energy discrimination is attainable with CsI-coated MCPs.[32]

Negative affinity GaAsP photocathodes have been studied as potentially very high effieciency photocathodes at soft x-ray wavelengths.[33] However, because of their extreme fragility, little progress has been made to date in developing these photocathodes in detectors that are either windowless or have thin windows for use at soft x-ray wavelengths.

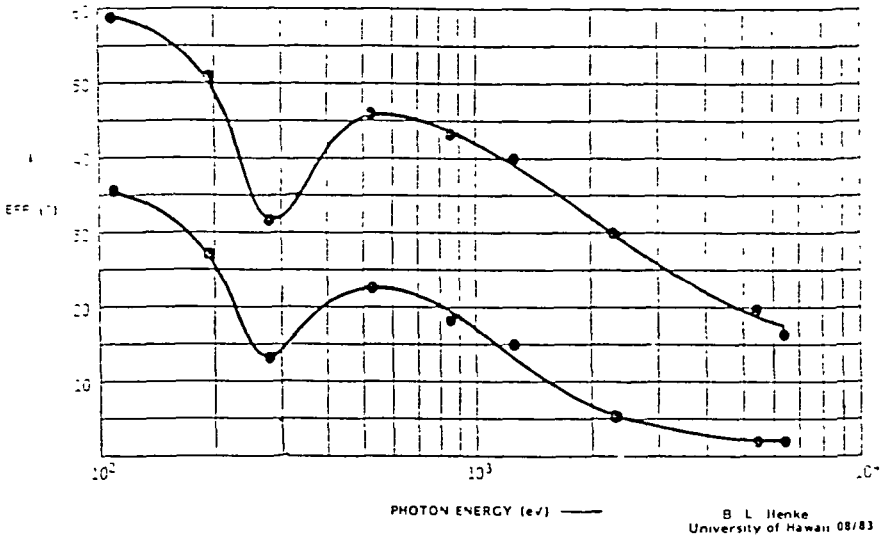

Figure 11. Quantum efficiencies of low-density ("fluffy") and high-density CsI photocathodes of optimum thickness illuminated at normal incidence (Henke [28]).

Comparison with CCDs

Development of the CCD detectors for astrophysical application is currently proceeding at a rapid rate.[34] Thinned, back-illuminated CCDs after ultraviolet flooding have demonstrated very high quantum efficiencies at blue and ultraviolet wavelengths and are currently under evaluation at x-ray wavelengths near 2Å. The development of large-format CCDs is also now in progress, and the delivery of the Textronix scientific CCD with 2048 x 2048 pixels on a 50 x 50 mm^2 active area is scheduled for early in 1986. The development of a deep depletion CCD for use at soft x-ray wavelengths has been discussed by a number of investigators (see for example, Walton *et al.*[35]).

Since there are a number of fundamental differences between the operating characteristics of the CCDs and the MCP detectors, the two classes of detectors are complementary and both are required for future astrophysics missions. Some of the more important differences for operation at soft x-ray wavelengths are listed in Table 1. First, the CCDs integrate charge on the chip and use a serial readout technique. For this reason, they are not suitable for applications which require fast timing of events. The electronic MCP detectors employ random readout systems, and events can be time-tagged to an accuracy equal to the pulse-pair resolution of the electronics. CCDs operate with gains ranging from ~30 to ~1600 at soft x-ray wavelengths and have a finite readout noise. The MCP detectors have gains of the order of 10^5 to 10^6 and operate with zero readout noise.

The most important advantage of the CCDs is that they can provide simultaneously a high-resolution imaging capability and a high level of energy resolution at soft x-ray wavelengths.[34,36] The MCP detectors can only provide, at best, a low level of energy resolution.

Table 1. Comparison of MCP and CCD Operating Characteristics at soft x-ray wavelengths

Parameter	MCP	CCD
Signal Integration	In external memory	On chip
Gain	10^5 to 10^6	~30 at 100 Å to ~1600 at 2 Å
Pulse-Counting	Yes	Yes (~8 Å)
Readout Noise	Zero	10 electrons rms
Event Timing Accuracy	100 ns	> 1 s for low-noise operation
Wavelength Response	Relatively narrow--tailored by photocathode material	Very broad (thinned and UV flood)
Sensitivity	soft x-ray and EUV - very high Ultraviolet - high Blue - moderate Red - low	Very high from soft x-ray to near infrared
Energy Resolution	Low	Very high
Cooling Requirements	Soft x-ray photocathodes --none	Below -100°C for low-noise operation
Sensitivity to Cosmic Rays	Low	High--thick chips Moderate--thinned chips

The key problem in the use of CCDs in astrophysical investigations at soft x-ray wavelengths is the elimination of long wavelength scattered radiation. The very broad wavelength response of the CCD is shown in Figure 12. For cool stars such as the sun the flux at ultraviolet and visible wavelengths is many orders of magnitude larger than the flux at soft x-ray wavelengths (see Figure 13) . Rejection of this longer wavelength scattered radiation requires the use of carbon filters for ultraviolet suppression even with the CsI-coated MCP detectors.

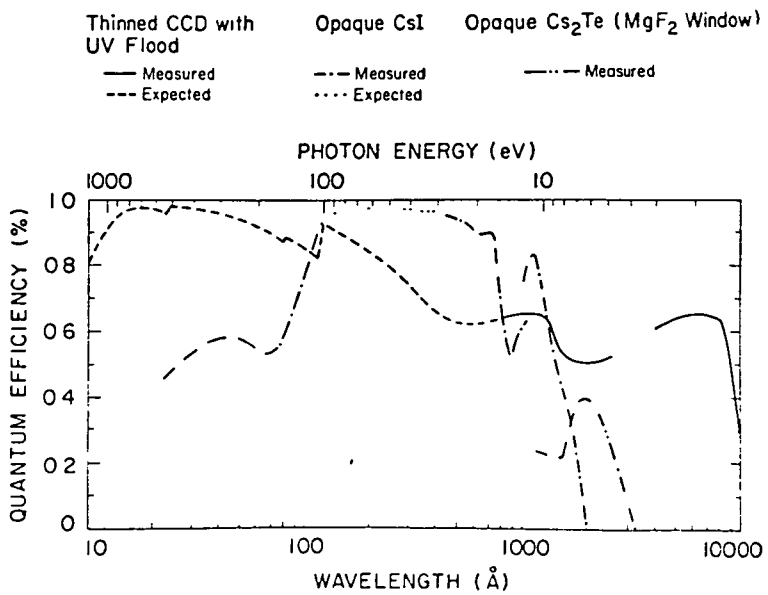

Figure 12. Quantum efficiencies of a thinned CCD with UV flood and of ultraviolet, EUV and soft x-ray photoemissive catnodes. (CCD data from Janesick et al.[34]; CsI and Cs_2Te data from Lukirskii et al.[29] ; Metzger[37] ; and Carruthers[38]).

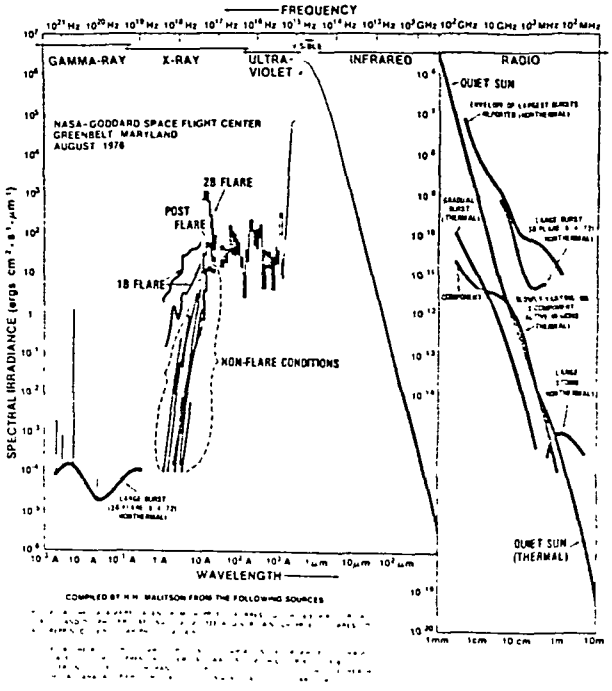

Figure 13. The solar spectrum.

Future Developments

Fueled by the requirements of high-volume civilian and military image-intensifier markets the MCP industry appears to be on a stable basis in the near future in the USA. In addition, several large-format MCP detector systems are being developed specifically for use on a number of NASA flight missions. Open-structure EUV and soft x-ray WSA detectors are being developed for imaging and spectroscopy on the EUV Explorer spacecraft by the group at the University of California, Berkeley.[39] The Smithsonian Astrophysical Observatory are fabricating a copy of the Einstein HRI for Rosat and are starting the development of an improved HRI with an active area of 100 x 100 mm^2 for the Advanced X-ray Astrophysics Facility (AXAF).[40] At Stanford, we are collaborating with Ball Aerospace Systems Division on the development of (2048 x 2048)- pixel MAMA detectors with active areas of 50 x 50 mm^2 (see Figure 14) for the NASA Goddard Hubble Space Telescope Imaging Spectrograph. In addition, we are starting the definition of an open-structure (256 x 16K)-pixel MAMA detector (see Figure 15) for use in the prime spectrograph of the Far Ultraviolet Spectroscopic Explorer (FUSE). As the result of these development programs we can expect further significant improvements in the performance characteristics of imaging MCP detector systems at soft x-ray wavelengths in the near future.

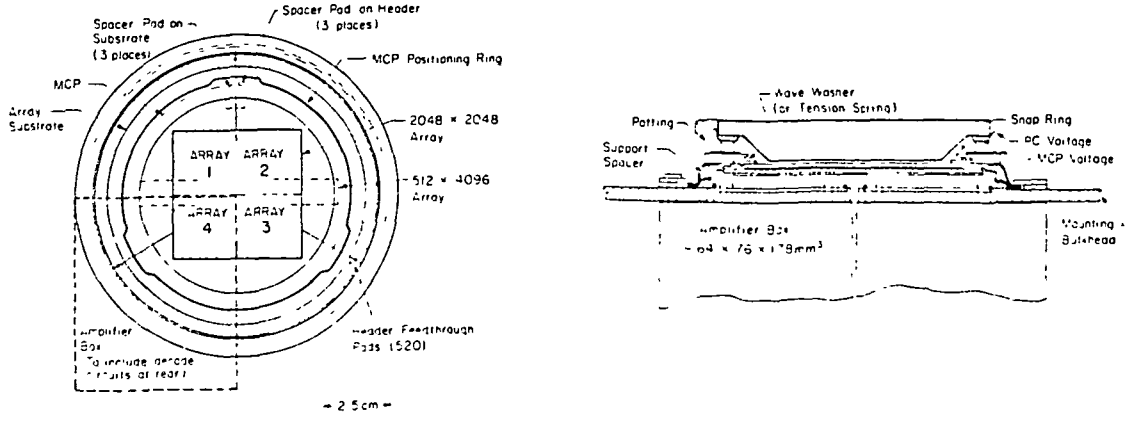

Figure 14. (2048 x 2048)-pixel MAMA detector for the Hubble Space Telescope Imaging Spectrograph.

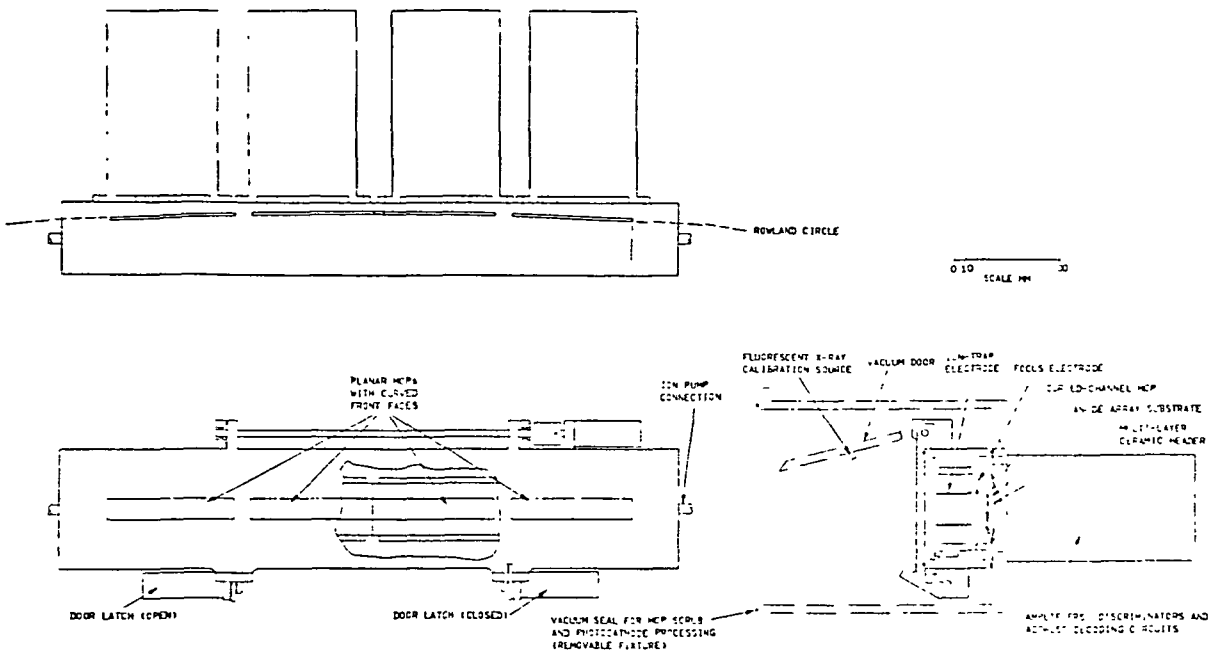

Figure 15. (256 x 16K)-pixel MAMA detector for the prime spectrograph of the Far Ultraviolet Spectroscopic Explorer (FUSE).

Acknowledgements

I am extremely grateful to the many individuals who freely provided the information collected in this review. The development of the soft x-ray MAMA detectors at Stanford University is supported by NASA Grant NAG5-622.

References

1. Wiza, J. L., Nuclear Instruments and Methods, Vol. 162, p. 587. 1979.
2. Siegmund, O. H. W., S. Clothier, J. Thornton, J. Lemen, R. Harper, I. M. Mason, and J. L. Culhane, IEEE Transactions on Nuclear Science, Vol. NS-30, p. 503. 1983.
3. Fraser, G. W., J. F. Pearson, G. C. Smith, M. Lewis, and M. A. Barstow, IEEE Transactions on Nuclear Science, Vol. NS-30, p. 455. 1983.
4. Timothy, J. G., Rev. Sci. Instrum., Vol. 52, p. 1131. 1981.
5. Galileo Electro-Optics Corporation, Sturbridge, MA 01518, USA.
6. E.G. and G. Reticon , Sunnyvale, CA 94086, USA.
7. Hartig, G. F., H. W. Moos, R. Pembroke, and C. Bowers, SPIE Instrumentation in Astronomy IV, Vol. 331, p. 45. 1982.
8. Williams, J. T., and D. Weistrop, SPIE Instrumentation in Astronomy V, Vol. 445, p. 204. 1983.
9. Stapinski, T. E., A. W. Rodgers, and M. J. Ellis, Pub. Astron. Soc. Pacific, Vol. 93, p. 242. 1981.
10. Latham, D. W., "Instrumentation for Astronomy with Large Optical Telescopes," IAU Colloquium, No. 67, C. M. Humphries, ed., (Boston, D. Reidel), p. 259. 1982.
11. Gornam, R., A. Rodgers, and T. Stapinski, SPIE Instrumentation in Astronmy IV, Vol. 331, p. 490. 1982.
12. Firmani, C., E. Ruiz, C. W. Carlson, M. Lampton, and F. Paresce, Rev. Sci. Instrum., Vol. 53, p. 570. 1982.
13. Firmani, C., L. Gutierrez, E. Ruiz, G. F. Bisiacchi, L. Salas, F. Paresce, C. W. Carlson, and M. Lampton, Astronomy and Astrophysics, Vol. 134, p. 251. 1984.
14. Kellogg, E., P. Henry, S. Murray, L. van Speybroeck, and P. Bjorkholm, Rev. Sci. Instrum., Vol. 47, p. 282. 1978.
15. Martin, C., P. Jelinsky, M. Lampton, R. F. Malina, and H. O. Anger, Rev. Sci. Instrum., Vol. 52, p. 1067. 1981.
16. Timothy, J. G., Optical Engineering, Vol. 24, p. 1066. 1985.
17. Lampton, M., and F. Paresce, Rev. Sci. Instrum., Vol. 45, p. 1098. 1974.
18. Parkes, W., K. D. Evans, and E. Mathieson, Nuclear Instruments and Methods, Vol. 121, p. 151. 1974.

19. Lampton, M., and C. W. Carlson, Rev. Sci. Instrum., Vol. 50, p. 1093. 1979.
20. Mertz, L. N., T. D. Tarbell, and A. M. Title, Applied Optics, Vol. 21, p. 628. 1982.
21. Schwartz, H. E., and J. S. Lapington, IEEE Transactions on Nuclear Science, Vol. NS-32, p. 433. 1985.
22. Ball Aerospace Systems Division, Boulder, Co 80306, USA.
23. Timothy, J. G., and R. L. Bybee, SPIE Shuttle Pointing of Electro-Optical Experiments, Vol. 265, p. 93. 1981.
24. Timothy, J. G., IEEE Transactions on Nuclear Science, Vol. NS-32, p. 427. 1985.
25. Fraser, G. W., M. A. Barstow, J. F. Pearson, M. J. Whiteley, and M. Lewis, Nuclear Instruments and Methods, Vol. 224, p. 272. 1984.
26. Whiteley, M. J., J. F. Pearson, G. W. Fraser, and M. A. Barstow, Nuclear Instruments and Methods, Vol. 224, p. 287. 1984.
27. Taylor, R., M. Hettrick, and R. F. Malina, Rev. Sci. Instrum., Vol. 54, p. 171. 1983.
28. Henke, B. L., private communication, 1983.
29. Lukirskii, A. P., F. P. Savinov, I. A. Brytov, and Y. F. Shepelev, USSR Acad. Sci. Bull Phys., Vol. 128, p. 774. 1964.
30. Fraser, G. W., M. A. Barstow, M. J. Whiteley, and A. Wells, Nature, Vol. 300, p. 509. 1982.
31. Tassano, P. L., J. Vac. Sci. Technology, Vol. A3, p. 2036. 1985.
32. Fraser, G. W., and J. F. Pearson, Nuclear Instruments and Methods, Vol. 219, p. 199. 1984.
33. Bardas, D., E. Kellogg, S. Murray, and R. Erickson Jr., Rev. Sci. Instrum., Vol. 49, p. 1273. 1978.
34. Janesick, J. R., T. Elliott, S. Collins, H. Marsh, M. M. Blouke, and J. Freeman, SPIE State-of-the-Art Imaging Arrays and their Applications, Vol. 501, p. 2. 1984.
35. Walton, D., R. A. Stern, R. C. Catura, and J. L. Culhane, SPIE State-of-the-Art Imaging Arrays and their Applications, Vol. 501, p. 306. 1984.
36. Janesick, J. R., these proceedings.
37. Metzger, P. H., J. Phys. Chem. Solids, Vol. 26, p. 1879. 1965.
38. Carruthers, G. R., SPIE Ultraviolet and Vacuum Ultraviolet Systems, Vol. 279, p. 112. 1981.
39. Hettrick, M. C., S. Bowyer, R. F. Malina, C. K. Martin, and S. Mrowka, Applied Optics, Vol. 24, p. 1737. 1985.
40. Murray, S. S., these proceedings.

CENTER FOR SPACE SCIENCE AND ASTROPHYSICS
Electronics Research Laboratory
Stanford University
Stanford, CA 94305